Practical Iterative Learning Control Considering Robust Stability for Fast and Precise Positioning of Galvano Scanner

Yoshihiro MAEDA
Department of Electrical and
Mechanical Engineering
Nagoya Institute of Technology
Gokiso, Showa, Nagoya 4668555, JAPAN
Email: ymaeda@nitech.ac.jp

Makoto IWASAKI
Department of Electrical and
Mechanical Engineering
Nagoya Institute of Technology
Gokiso, Showa, Nagoya 4668555, JAPAN
Email: iwasaki@nitech.ac.jp

***Abstract*—This paper presents an iterative learning control (ILC) design technique for the fast and precise positioning of galvano scanners with parameter fluctuations. ILC scheme is well-known as a strong control approach for high-precision motion control of mechatronic systems. However, since ILC is heavily sensitive to modeling errors and uncertainty, resonant frequency fluctuations in the galvano scanner greatly affect stability of ILC and deteriorate the learning control performance. In this study, therefore, an ILC approach using zero phase error notch filters is presented to improve the control performance with the ILC stability robustly satisfied. Effectiveness of the proposed ILC has been verified by numerical simulations using a galvano scanner.**

I. Introduction

In a wide variety of high performance industrial mechatronic systems such as data storage devices, machine tools, and industrial robots, the fast-response and high-precision positioning control is one of indispensable techniques for high productivity and/or high quality of products [1]. However, such mechatronic systems cause parameter fluctuations (e.g., torque constant of actuator, resonant frequency, and moment of inertia) due to changes of environment temperature, aging, etc, which deteriorate the motion control performance.

In order to overcome the above issue, iterative learning control (ILC) may be one of the effective approaches, and a variety of ILC methods have been proposed in the former literature, e.g., PD-type and tunable designs [2], system inversion methods [3]-[5], $\mathcal{H}_\infty$ methods [6], and quadratically optimal designs [7]. ILC learns only the repetitive disturbances and ignores noise and non-repetitive disturbances, and the system inversion methods [3]-[5] can quickly converge the learning function in the above methods. Therefore, if effects of the parameter fluctuations can be regarded as the repetitive disturbances, then ILC can compensate the deterioration of the positioning performance. However, it is well-known that ILC is quite sensitive to modeling errors and uncertainties [6], [7], which makes it difficult to apply to the fast and precise positioning control. For instance, in a case of galvano scanners for laser manufacturing machines, mechanical resonant vibrations restrict ILC performance.

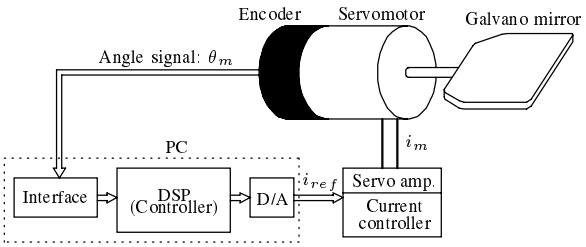

Fig. 1. Configuration of galvano scanner control system.

In this study, a practical and effective system inversion-based ILC design for resonant systems is presented to obtain the robust fast and precise positioning performance of galvano scanners. Before ILC design, effects of the parameter fluctuations are analyzed in detail and it is clarified that the fluctuation of the resonant frequencies distinctively affects stability of ILC. Then, zero phase error notch filters are presented as a learning filter of ILC to ensure sufficient stability for the resonant modes and to extend the control bandwidth. Effectiveness of the proposed ILC design has been demonstrated by numerical simulations using a prototype of galvano scanner, in comparison with the conventional ILC design using a simple lowpass filter.

II. Galvano Scanner Control System

A. System Configuration

Fig. 1 shows a configuration of a laboratory positioning device for a galvano scanner in laser manufacturing machines [1]. The galvano scanner is composed of a DC servomotor with a galvano mirror on the shaft, and the motor angle θ_m is directly detected by a rotary encoder (resolution of 1.498×10^{-6} rad/pulse) on the shaft. The detected angle θ_m is transferred to a DSP through an interface with the sampling period of $T_s = 20$ μs. The servomotor is driven by a current-

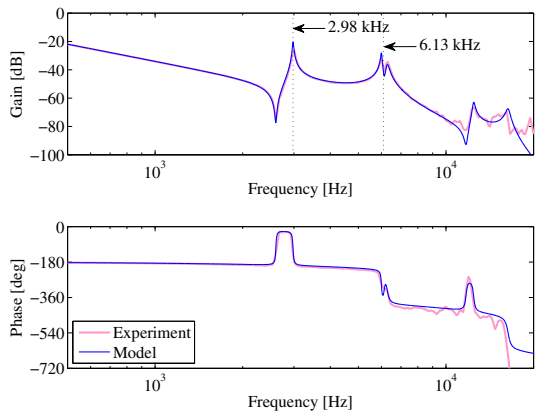

Fig. 2. Bode plots of plant system.

controlled linear amplifier (control bandwidth of 20 kHz) with the current reference i_{ref} generated by the position controller. This position control system, therefore, operates the galvano scanner as a typical semi-closed control system.

B. Frequency Characteristic

Light solid lines in Fig. 2 indicate an experimental Bode plot of θ_m for i_{ref} as the control input. From the figure, the mechanism includes the primary resonant mode at 2.98 kHz, the second resonant mode at 6.10 kHz, other resonant modes in the higher frequency range over 10 kHz, and a dead time component due to the current control delay and the digital-to-analog (D/A) conversion. The following polynomial is a nominal plant model $P(s) = \theta_m(s)/i_{ref}(s)$, consisting of a rigid mode, resonant modes up to $l = 5$, and a dead-time component:

$$P(s) = e^{-Ls} K_p \left(\frac{1}{s^2} + \sum_{l=1}^{5} \frac{k_l}{s^2 + 2\zeta_l \omega_l s + \omega_l^2} \right), \qquad (1)$$

where $K_p (= K_t K_c / J)$ is the gain including moment of inertia J, torque constant of motor K_t, and steady gain of the current control system K_c, ω_l is the natural angular frequency of l-th resonant mode, ζ_l is the damping coefficient, k_l is the resonant mode gain, and L is the equivalent dead time, respectively. Dark solid lines in Fig. 2 indicate a Bode plot of $P(s)$, which well-reproduces the experimental plant characteristic.

It has been confirmed by experiments using the target galvano scanner that the torque constant K_t, the primary resonant frequency $f_1 (= \omega_1/2\pi)$, and the second resonant frequency $f_2 (= \omega_2/2\pi)$ fluctuate due to environment temperature, heating, and aged deterioration [1]. The maximum fluctuation from the nominal parameter is ± 3 % in K_t, ± 100 Hz in f_1, and ± 200 Hz in f_2, respectively. The fluctuation of f_1 and f_2 remarkably affect the frequency characteristic of the plant, and deteriorates the system stability [8]. In addition, there are some uncertainties in the frequency range over 10 kHz.

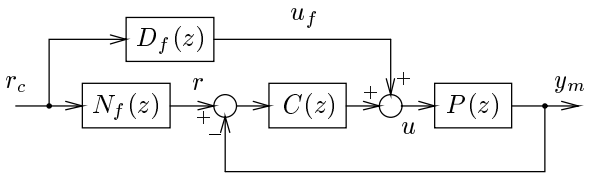

Fig. 3. Block diagram of 2DoF position control system.

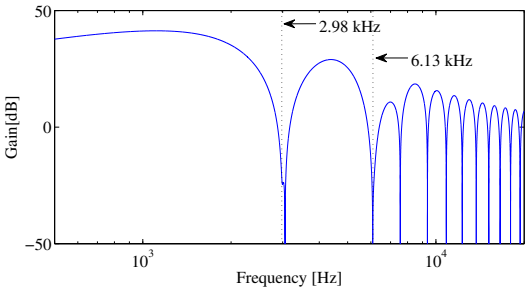

Fig. 4. Gain characteristic of $D_f(z)$.

C. Target Control Specification

In this research, a target position reference with the stroke of 1.5 mm in the laser position (1 mm in the laser position corresponds to 0.0067 rad in the motor angle) is given as a typical specification for actual manufacturing in industry. The motor position should follow the target position with the accuracy within ± 3 μm by the settling time of 0.72 ms$(= 36T_s)$. Achieving the target positioning performance is very challenging, since the required response frequency is about 1.38 kHz$(= 1/0.00072)$ that is quite close to the primary resonant frequency $f_1 = 2.98$ kHz (normally, the response frequency is set to less than one-fifth from one-third of the primary resonant frequency.)

D. Position Control System

Fig. 3 shows a block diagram of two degree-of-freedom (2DoF) position control system, where $N_f(z)$ and $D_f(z)$ are the FF controllers, $C(z)$ is the FB controller, $P(z)$ is the discrete-time plant model of $P(s)$ in eq.(1) with a zeroth-order hold, r_c is the target position reference, r is the target position trajectory reference, $y_m(z)$ is the motor position in linear scale, u_f is the FF control input, and u is the current reference i_{ref} as the control input, respectively. $N_f(z)$ and $D_f(z)$ are designed on the basis of the deadbeat control framework [8] with the aim at suppressing the residual vibration due to the primary and secondary vibration modes. Fig. 4 shows a gain characteristic of the FF controller $D_f(z)$. From the figure, $D_f(z)$ attenuates frequency components around 2.98 kHz and 6.13 kHz in u_f, to suppress the residual vibration in y_m. On the other hand, $C(z)$ is composed of a phase lag-lead compensator and two notch filters for robustly stabilizing the primary and second vibration modes.

In order to clarify influence of the plant parameter fluctuations for the positioning motion, simulated response wave-

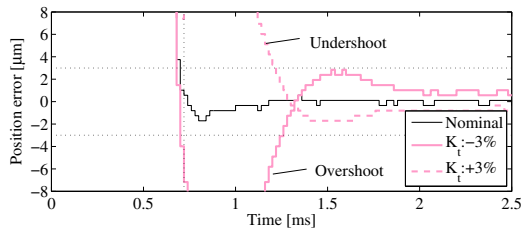

(a) fluctuation of K_t

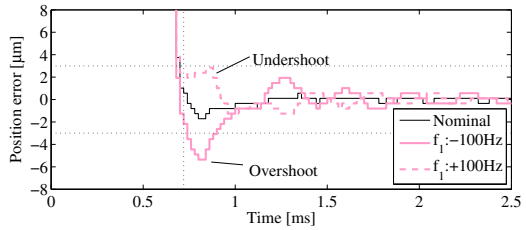

(b) fluctuation of f_1

Fig. 5. Simulation results for 1.5 mm stroke positioning with parameter fluctuations of K_t and f_1.

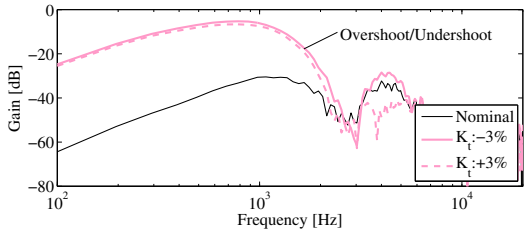

(a) fluctuation of K_t

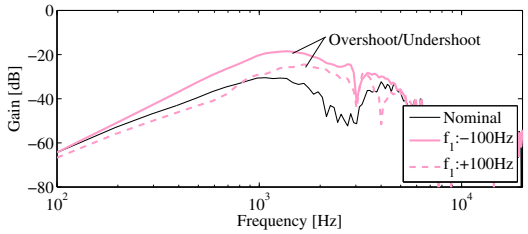

(b) fluctuation of f_1

Fig. 6. Frequency characteristics of position tracking error.

forms of the position error $r_c - y_m$ for 1.5 mm stroke positioning motion are indicated in Fig. 5. Fig. 5(a) shows the simulation results with the fluctuation of K_t, while Fig. 5(b) shows the ones with the fluctuation of f_1, respectively. From Fig. 5(a), the fluctuation of K_1 causes remarkable overshoot/undershoot responses around the target position, which deteriorates the target settling accuracy of ± 3 μm indicated by horizontal dotted lines. On the other hand, in the cases of the fluctuation of f_1, although the residual vibration can be successfully suppressed within ± 3 μm by the FF compensation, the overshoot/undershoot responses with the maximum amplitude of 5.4 μm cause just after the target settling time of 0.72 ms. Fig. 6(a) and Fig. 6(b) show the frequency characteristics of $r - y_m$. From the figures, frequency components of the overshoot/undershoot in the cases of the fluctuations of K_t and f_1 are mainly less than $2 \sim 3$ kHz that corresponds to the required response frequency defined in II-C. Therefore, in order to improve the positioning accuracy even if the plant parameter fluctuations exist, suppressing the response variation with the frequency components of less than $2 \sim 3$ kHz would be effective.

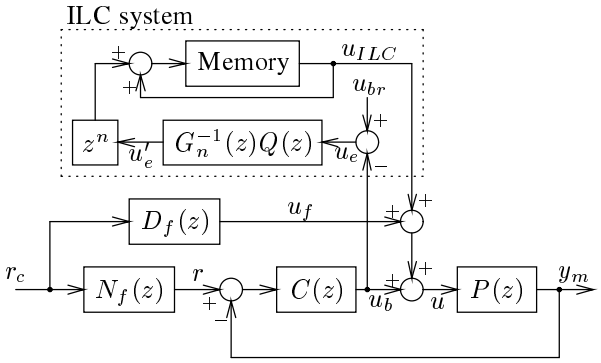

Fig. 7. Block diagram of 2DoF position control system with ILC system.

III. Iterative Learning Control for Galvano Scanner

In this section, a basic time-domain iterative learning control is designed as a conventional method, with consideration of the response variation due to the parameter fluctuations. Then, it is clarified by simulation analyses that the fluctuations of the resonant frequencies drastically deteriorate the stability of the ILC system and restrict the ILC performance.

A. ILC System

Fig. 7 shows a block diagram of 2DoF position control system with an ILC system, where u_b is the FB control input calculated by $C(z)$, u_{br} is the target FB control input in ILC, $u_e = u_{br} - u_b$ is the FB control input error, u_{ILC} is the learning control input as the ILC system output, $Q(z)$ is the learning filter, $G_n(z)$ is the nominal transfer characteristic of u_b for u_{ILC}, and z^n is the forward time-shift operator that compensates the time delay of u'_e due to calculation of $Q(z)G_n^{-1}(z)$, respectively. In this study, the system inversion $G_n^{-1}(z)$ is realized on the basis of the zero phase error control scheme [9], and the time delay due to unstable zeros of $G_n(z)$ is two samples ($2T_s$).

Firstly, the error u_{e1} in the first iteration is expressed as

$$u_{e1}(z) = u_{br}(z) - u_{b1}(z) = u_{br}(z) - G(z)u_{ILC1}(z), \quad (2)$$

where the number of the subscript in each variable means the iteration number and u_{ILC1} is defined as zero. Next, u_{ILC2} in the second iteration is given as

$$u_{ILC2}(z) = u_{ILC1}(z) + z^n G_n^{-1}(z)Q(z)u_{e1}(z). \quad (3)$$

Therefore, the general relationship of u_e between k-th and $(k+1)$-th iterations can be expressed by the following equation.

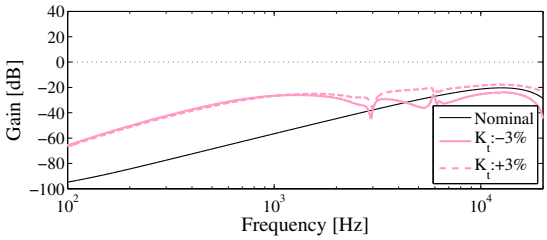

(a) fluctuation of K_t

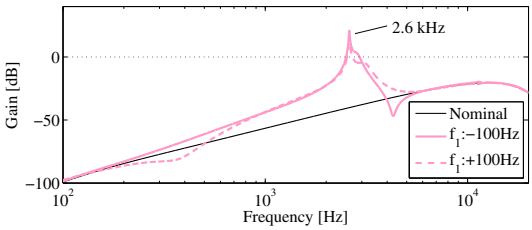

(b) fluctuation of f_1

Fig. 8. Stability characteristics of ILC system under $Q(z) = 1$.

$$u_{e(k+1)}(z) = \{1 - z^n G(z) G_n^{-1}(z) Q(z)\} u_{ek}(z) \tag{4}$$

Here, by defining $G(z)$ as $G(z) = G_n(z)\Delta(z)$, the stable condition of the ILC system can be stated as

$$|1 - z^n \Delta(z) Q(z)| < 1. \tag{5}$$

Note that when eq.(5) is satisfied, u_e converges to zero by repeating the iteration, and as a result, y_m precisely follow to r under $u_{br} = 0$. In addition, it is clear that $Q(z)$ should be carefully designed with consideration of the effect of $\Delta(z)$ [3]-[7].

B. Stability Analysis for Parameter Fluctuations

In order to examine effects of the plant parameter fluctuations and clarify the problem for applying ILC to the galvano scanner, the stability of ILC system is analyzed by simulations under $Q(z) = 1$. In this simulation analysis, the torque constant K_t is fluctuated by ± 3 % and the primary resonant frequency f_1 is fluctuated by ± 100 Hz, respectively. Fig. 8 shows stability characteristics $|1 - z^n \Delta(z) Q(z)|$. In the case that K_t fluctuates ± 3 % as shown in Fig. 8(a), ILC is stable since the gain is less than 0 dB in all frequency range. On the other hand, in the case that f_1 fluctuates ± 100 Hz as shown in Fig. 8(b), ILC cannot satisfy the stable condition around a frequency of 2.6 kHz that corresponds to the anti-resonant frequency of the primary vibration mode. Therefore, it is clarified by the stability analysis that the ILC system has less robust stability against the fluctuation of f_1.

Note that since the fluctuation of the second resonant frequency f_2 also deteriorates the stability, $Q(z)$ should decrease the gain around the primary and second resonant modes in the system inversion ILC scheme. In this study, the target gain of $|1 - z^n \Delta(z) Q(z)|$ is required as less than -100 dB around the resonant modes to stabilize ILC.

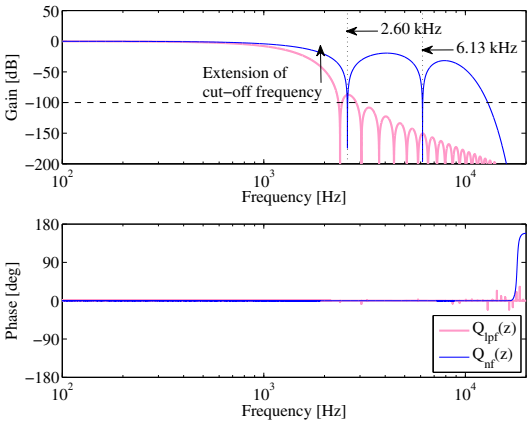

Fig. 9. Bode plots of learning filters.

IV. ILC Filter Design for Stabilizing Resonant Vibration Modes

In this section, we design two learning filters: one is a low-pass filter as the conventional approach. Another is a low-pass and notch filter as the proposed approach. Both filters are FIR-type filters to realize a linear phase delay property with consideration of the forward time-shift operator z^n shown in Fig. 7.

A. Zero Phase Error Low-pass Filter

A low-pass filter $Q_{lpf}(z)$ for ILC is designed on the basis of the window function that is one of the popular and useful techniques in the digital filter design. $Q_{lpf}(z)$ can be defined by the following FIR filter:

$$Q_{lpf}(z) = \frac{a_0 z^N + a_1 z^{N-1} + \cdots + a_{N-1} z + a_N}{z^N}, \tag{6}$$

where the coefficients $a_k (k = 0, \ldots, N)$ equal to a finite impulse response of the desired frequency response at $t = kT_s$. In addition, a_k satisfies the following relationship so that $Q_{lpf}(z)$ possesses a linear phase property [9]:

$$a_k = a_{N-k}, \tag{7}$$

where if N is odd number, then $k = 0, \ldots, (N-1)/2$, else $k = 0, \ldots, N/2 - 1$. respectively. From eqs. (6) and (7), $Q_{lpf}(z)$ is expressed as follows:

$$Q_{lpf}(z) = \frac{a_0 z^N + a_1 z^{N-1} + \cdots a_1 z + a_0}{z^N}. \tag{8}$$

In order to possess robust stability against the resonant frequency fluctuations, the cut-off frequency of the desired frequency property is assigned to 1.2 kHz with consideration of the control bandwidth of ILC. Note that the humming window is utilized as a window function in the filter design. The order N of $Q_{lpf}(z)$ is set to 50 and fourth power of $Q_{lpf}(z)$ is defined as the final filter, i.e., $Q_{lpf}(z) := Q_{lpf}(z)^4$. The order of the designed $Q_{lpf}(z)$, therefore, becomes 200. Light lines in Fig. 9 show Bode plots of $Q_{lpf}(z)$. From the figure, $Q_{lpf}(z)$ attenuates the gain around the primary and

second resonant modes less than 100 dB, and realizes a zero phase property (in this case, z^{100} is multiplied to $Q_{lpf}(z)$ to compensate the time delay). On the other hand, since the cut-off frequency (i.e., a frequency where the gain attenuates less than 3 dB) is 647 kHz, the response variation over the frequency may not be suppressed sufficiently.

B. Zero Phase Error Notch Filter

In order to achieve higher control bandwidth than $Q_{lpf}(z)$ with satisfying the robust stability against the resonant frequency fluctuations, we design an advanced ILC filter $Q_{nf}(z)$ using notch filters that shapely attenuate frequency components around the target resonant modes. An FIR filter that possesses a linear phase property and zero-damping, i.e., zeros are on the unit circle in complex plane, has the following zeros:

$$z_n = e^{j\omega_{nf}T_s}, \bar{z_n} = e^{-j\omega_{nf}T_s}, \omega_{nf} = 2\pi f_{nf}, \tag{9}$$

where f_{nf} is the damping frequency and $\bar{z_n}$ expresses a conjugate complex number of z_n. A notch filter $Q_{nf}(z)$ with the zeros of z_n and $\bar{z_n}$ can be defined as

$$\begin{aligned} Q_{nf}(z) &= (z^{-1} - z_n)(z^{-1} - \bar{z_n}) &(10)\\ &= \frac{z_n\bar{z_n}z - (z_n + \bar{z_n}) + z^{-1}}{z} = \frac{N_{nf}(z)}{D_{nf}(z)}. &(11)\end{aligned}$$

Here, the frequency characteristic of $N_{nf}(z)$ is expressed as follows, by substituting $z = e^{j\omega T_s}$ to $N_{nf}(z)$:

$$\begin{aligned} N_{nf}(z) &= e^{j\omega_m T_s}e^{-j\omega_m T_s}e^{j\omega T_s} \\ &\quad -(e^{j\omega_m T_s} + e^{-j\omega_m T_s}) + e^{-j\omega T_s} \\ &= 2\cos\omega T_s - 2\cos\omega_m T_s \end{aligned} \tag{12}$$

It is obvious that $Q_{nf}(z)$ has a linear phase property since the numerator $N_{nf}(z)$ does not include complex components. In addition, $Q_{nf}(z)$ becomes zero at $\omega = \omega_m$.

On the basis of the above mentioned zero phase error notch filter design, we design an ILC filter $Q_{nf}(z)$ for the galvano scanner. In order to make the ILC system stable for the primary and second vibration modes, zeros of the notch filter are assigned as follows:

$$\begin{aligned} z_1 &= e^{j\omega_{nf1}T_s}, \bar{z_1} = e^{-j\omega_{nf1}T_s}, \omega_{nf1} = 2\pi f_{nf1}, &(13)\\ z_2 &= e^{j\omega_{nf2}T_s}, \bar{z_2} = e^{-j\omega_{nf2}T_s}, \omega_{nf2} = 2\pi f_{nf2}, &(14)\\ z_3 &= e^{j\omega_{nf3}T_s}, \omega_{nf3} = 2\pi f_{nf3}. &(15)\end{aligned}$$

Eqs. (13) and (14) impose notch filters for the primary and second resonant modes for achieving the robust stability, while eq.(15) means a low-pass filter with a zero at Nyquist frequency $f_{nf3} = 1/2T_s$, respectively. Therefore, each filter that includes the specified zeros and makes the steady gain unity can be mathematically formulated as follows:

$$\begin{aligned} Q_{nf1}(z) &= \frac{z_1\bar{z_1}z - (z_1 + \bar{z_1}) + z^{-1}}{|2 - z_1 - \bar{z_1}|z}, &(16)\\ Q_{nf2}(z) &= \frac{z_2\bar{z_2}z - (z_2 + \bar{z_2}) + z^{-1}}{|2 - z_2 - \bar{z_2}|z}, &(17)\\ Q_{nf3}(z) &= \frac{z - z_3}{|1 - z_3|z}. &(18)\end{aligned}$$

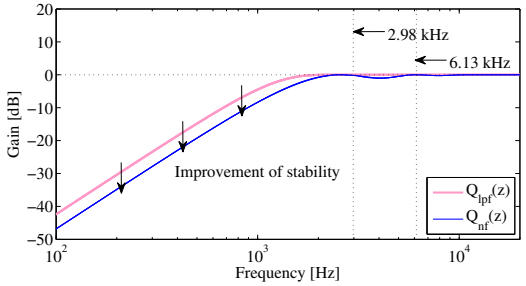

Fig. 10. Stability characteristics of ILC systems with $Q_{lpf}(z)$ and $Q_{nf}(z)$.

Finally, the proposed ILC filter $Q_{nf}(z)$ can be expressed as follows, by connecting multi-powered $Q_{nf1}(z)$, $Q_{nf2}(z)$, and $Q_{nf3}(z)$:

$$Q_{nf}(z) = Q_{nf1}(z)^{K_1}Q_{nf2}(z)^{K_2}Q_{nf3}(z)^{K_3}. \tag{19}$$

The damping frequencies of f_{nf1} and f_{nf2} are determined as $f_{nf1} = 2.60$ kHz and $f_{nf2} = 6.13$ kHz, with consideration of the stability of ILC as explained in III-B. On the other hand, the parameters K_1, K_2, and K_3 are assigned as $K_1 = 2$, $K_2 = 2$, and $K_3 = 52$ by trial and error so that $Q_{nf}(z)$ has sufficient robust stability and low-pass property in the high frequency range over 10 kHz. As a result, the order of $Q_{nf}(z)$ becomes 60.

Bode plots of $Q_{nf}(z)$ is indicated by dark lines in Fig. 9. From the figure, $Q_{nf}(z)$ extends the bandwidth with comparison to $Q_{lpf}(z)$ (i.e., the cut-off frequency is 647 Hz $\rightarrow$ 850 Hz). In addition, the gain is sharply attenuated at the specified frequencies f_{nf1} and f_{nf2}.

C. Analysis of Robust Stability and Disturbance Suppression Property

The robust stability against the plant parameter fluctuation are comparatively analyzed by using $Q_{lpf}(z)$ and $Q_{nf}(z)$ designed in IV-A and IV-B. In the numerical analysis, the primary resonant frequency f_1 is fluctuated by ± 100 Hz as an example, which is the most sensitive parameter for the ILC stability. Fig. 10 shows stability characteristics of the ILC systems with $Q_{lpf}(z)$ and $Q_{nf}(z)$. From the figure, both filters can suppress the gains less than 0 dB and satisfy the robust stability. It has been confirmed by simulations that both filters can make the ILC system stable in the cases of $K_t : \pm 3$ % or $f_2 : \pm 200$ Hz. On the other hand, the sensitivity gain less than 2 kHz is further decreased by $Q_{nf}(z)$ in a maximum of 6 dB, which leads to an improvement of the disturbance suppression in the frequency range.

V. Simulation Verification

Effectiveness of the proposed ILC approach is comparatively evaluated by numerical simulations for the fast and precise positioning of the galvano scanner. Here, the parameter fluctuations are set as $K_t : -3\%$, $f_1 : -100$ Hz, and $f_2 : -200$ Hz, which is the most tough situation for the ILC stability. Fig. 11 shows response waveforms of (a) position

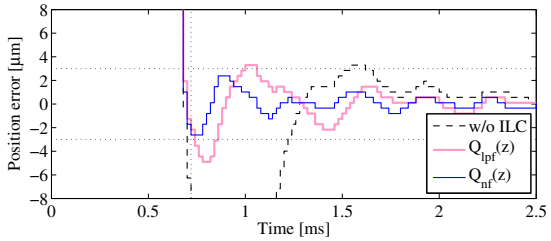

(a) Position error $r_c - y_m$

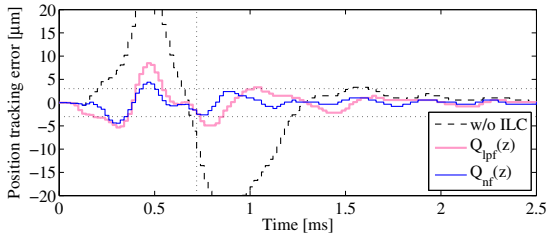

(b) Position tracking error $r - y_m$

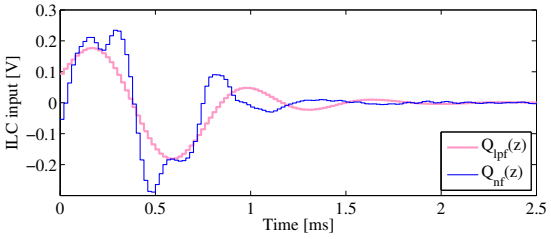

(c) ILC input u_{ILC}

Fig. 11. Simulation results for 1.5 mm stroke positioning with parameter fluctuations of K_t and f_1.

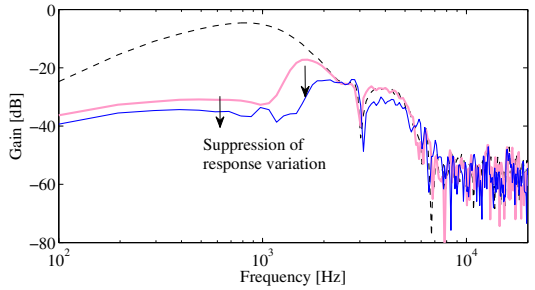

Fig. 12. Frequency characteristics of position tracking error.

error $r_c - y_m$, (b) position tracking error $r - y_m$, and (c) ILC input u_{ILC} in the tenth iteration (i.e., tenth positioning trial). Note that learning of ILC has been sufficiently converged during ten times of positioning trials.

From the figure, both ILC filters possess the robust stability against the parameter fluctuations and improve the positioning performance in comparison with the result without ILC. On the other hand, $Q_{nf}(z)$ reduces the position tracking error during the transient and suppresses the overshoot/undershoot displacement within ± 2.6 μm at the settling, in comparison with $Q_{lpf}(z)$. Fig. 12 shows a comparison of frequency characteristics of $r - y_m$, and $Q_{nf}(z)$ well-suppresses the frequency components of the response variation, especially at frequencies less than 2 kHz.

VI. Conclusion

This paper presented a practical and effective ILC design for the fast and precise position control of a galvano scanner with mechanical and electrical parameter fluctuations. The proposed ILC filter design stands on a simple notch filter design whose concept is widely known in industry, and can extend the control bandwidth of ILC with ensuring sufficient stability against the resonant modes. The positioning performance has been explicitly improved in comparison with the conventional ILC using a lowpass filter.

As a future work, we would like to evaluate the presented ILC by experiments using a galvano scanner, in which the plant parameters are actually varied by self-heating due to repetitive motion and/or changes of environment temperature. In addition, an advanced ILC filter design aiming at reduction of the order is also required for improving computational load and quick learning performance.

Acknowledgment

The authors would like to thank Via Mechanics, Ltd, for supporting experimental equipment.

References

[1] D. Matsuka, S. Fukushima, and M. Iwasaki, "Compensation for Torque Fluctuation Caused by Temperature Change in Fast and Precise Positioning of Galvanometer Scanners," in *Proc. 2015 IEEE Int. Conf. Mechatron.*, Nagoya, Japan, 2015, pp. 638–643.

[2] Y. M. Zhao, Y. Lin, F. Xi, and S. Guo, "Calibration-Based Iterative Learning Control for Path Tracking of Industrial Robots," IEEE Trans. Ind. Electron., vol. 62, no. 5, pp. 2921–2929, 2015.

[3] H. Elci, R.W. Longman, M. Phan, J.-N. Juang, and R. Ugoletti, "Discrete Frequency Based Learning Control for Precision Motion Control," in *Proc. IEEE Int. Conf. Syst., Man, Cybern.*, San Antonio, USA, 1994, pp. 2767–2773.

[4] T. Sogo, "Stable Inversion for Nonminimum Phase Sampled-Data Systems and its Relation with the Continuous-Time Counterpart," in *Proc. 41st IEEE Conf. Decision Contr.*, 2002, pp. 3730–3735.

[5] J. Ghosh and B. Paden, "Pseudo-Inverse Based Iterative Learning Control for Nonlinear Plants with Disturbances," in *Proc. 38th IEEE Conf. Decision Contr.*, Phoenix, USA, 1999, pp. 5206–5212.

[6] D. A. Bristow, M. Tharayil, and A. G. Alleyne, "A Survey of Iterative Learning Control -A Learning-Based Method for High-Performance Tracking Control-," *IEEE Cont. Syst. Mag.*, vol. 26, no. 3, pp. 96–114, 2006.

[7] D. Gorinevsky, "Loop Shaping for Iterative Control of Batch Processes," *IEEE Contr. Syst. Mag.*, vol. 22, no. 6, pp. 55–65, 2002.

[8] Y. Maeda and M. Iwasaki, "Improvement of Adaptive Property by Adaptive Deadbeat Feedforward Compensation Without Convex Optimization," *IEEE Trans. Ind. Electron.*, vol. 62, no. 1, pp. 466–474, 2015.

[9] M. Tomizuka, "Zero Phase Error Tracking Algorithm for Digital Control," *ASME J. Dyn. Syst., Meas., and Control*, vol. 109, pp. 65–87, Mar. 1987.